Journal of Sound and Vibration (1999) **222**(5), 723–752
Article No. jsvi.1998.2082, available online at http://www.idealibrary.com on IDEAL®

HIERARCHICAL CONTROL OF HYDRAULIC ACTIVE SUSPENSIONS OF A FAST ALL-TERRAIN MILITARY VEHICLE

J. DER HAGOPIAN AND L. GAUDILLER

Laboratoire de Mécanique des Structures-UPRES A 5006 *C.N.R.S.*, *Institut National des Sciences Appliquées*, 20 *avenue Albert Einstein*, 69621 *Villeurbanne*, *France*

AND

B. MAILLARD

D.G.A. E.T.A.S Etablissement Technique d'Angers, *route de Laval*, 49460 *Angers Cedex* 01, *France*

(*Received* 17 *March* 1998, *and in final form* 27 *October* 1998)

This paper describes a procedure to improve the behavior of a light all-terrain military vehicle moving, over rough ground and large obstacles, at high speed. This improvement has governed the choice of a new concept of hydraulic active–passive linking between the body and the ground. A hierarchical control strategy is then proposed which divides the management of vehicle dynamics into two levels: a central control which takes into account the pitch and the gap between the body and the ground and delivers orders to local independent controls devoted to each active suspension and bogie assembly. In this case, the feasibility of this control can be validated on a quarter vehicle moving only in the vertical direction. The local controller uses a classical P.I.D. and the central control implemented uses a Linear Quadratic Gaussian which is suited to the specific purposes of the control. A scale model of a quarter vehicle is used to validate this process. Simulation and experimental results are in good agreement and show the improvement of capacities for crossing large obstacles at speed.

1. INTRODUCTION

Off-highway vehicles must be able to clear the most difficult obstacles at high speed while maintaining both good vibratory insulation of the body and passenger safety. In addition, the fact that military vehicles must be capable of fast response in military operations requires high performance in terms of mobility.

The overall performance of the linking between the body and the ground contributes the most important parameter in the behavior of off-highway vehicles. It is connected primarily with three criteria: speed of translation which

0022–460X/99/200723 + 30 $30.00/0

provides the capacity to move over flat surfaces and slopes; maneuverability, making it possible to take bends at high speed; and agility which characterizes the ability to clear rough ground at high speed [1]. The improvement of the criteria governs the choice of the drive line, which should adjust to the ground, and the suspension, which should decrease the dynamic effects induced by the profile of the ground when the vehicle is moving [2].

The solutions proposed in the domain of mobile robotics allow increasing capability to cross over large obstacles at slow speed by adjusting the drive lines to the profile of the ground. Different works have shown that the amplitude of this speed is related to the number of degrees of freedom of the linking between the body and the ground. A compromise must be found between the number of degrees of freedom and the simplicity of suspension and locomotion design to increase speed when clearing the obstacles [3].

The improvement of these performances requires the use of new concepts [4–6]. The selection of the components of a passive suspension is the result of a compromise between the comfort of the passengers, the clearance of the suspension and the road-holding qualities [7]. Nevertheless the characteristics of the passive components are fixed and their performances are restricted since they can only store or dissipate energy [8].

Optimizing the characteristics of passive suspensions leads to the development of controlled suspensions [9–11] particularly in the domain of motor vehicles [11–13]. The concept of the combined controlled wheels and suspensions [14] meets the demands of the army for their future light off-highway vehicles. In fact, tracked drive lines or wheeled bogies increase clearance speed over large obstacles while controlled suspension leads to improved passenger comfort and control over movements of the vehicle body.

Controlled suspensions can be grouped in two categories: semi-active suspensions which make use of devices which, without supplying operational energy [15], modify the stiffness and the damping characteristics of the suspension, and active suspensions which use an external energy supply. These permit modifying the vehicle's suspension clearance and attitude [16, 17].

In the case of off-highway military vehicles it must be possible to modify the clearance between the ground and the body [18]. This consideration leads to the use of a combination in series of active and passive suspensions [19–21].

Since the sixties, the principles of active suspension control were first set out and expressed in the so-called "Skyhook" system [22]. Then the implementation of the state form and the techniques of Linear Quadratic control (L.Q.) were included to optimize control by using a quadratic criterion of the performances. Linear Quadratic Gaussian theory (L.Q.G.) is applied to reconstruct the non-measurable states. An observer [23] is then used [24].

However, the use of this reconstruction remains difficult in the case of suspensions and a sub-optimal solution obtained by a linear combination of measurements is preferred [25].

In this study, a new concept of linking the body and the ground for military off-highway vehicles is presented. This new concept uses bogie drive lines and a combination in series of active and passive suspensions driven by a hierarchical type control.

First a geometrical study of obstacle clearance is presented which leads to the choice of the type of drive line. Then, a study of the dynamic behavior of a classical suspension is made to show its limits with respect to the performances required from the off-highway vehicles of the future.

A hierarchical control, which includes the performance criteria, is then proposed to control the clearance between the body and the ground, the pitching, and the dynamic behavior of the whole vehicle. This hierarchical control has two levels composed of a central control which pilots local controls. The local controls act on each suspension.

This is followed by the theoretical study of the dynamic behavior of a quarter vehicle with this type of control. The quarter vehicle is composed of the quarter of the mass of the body mounted on the head of a hydraulic cylinder in series with a passive suspension and a two-wheel bogie. A model of the hydraulic cylinder is formulated. Simulations are carried out to adjust the parameters of the local control for speed and the central control.

Finally, an experimental set-up corresponding to the above quarter vehicle is presented. The modal parameters are identified and model tuning experiments are carried out. The results compared to those of the simulations are in good agreement. These results show the efficiency of this system and the validity of the choices made.

2. STUDY OF THE CROSSING OF LARGE OBSTACLES

The expected performances of the light military vehicles of the future are linked to the capacity of clearing large obstacles at high speed. In this case, the height of the obstacles is 0·35 times the diameter of the wheel and the speed of translation is about 17 m/s (35 miles per hour). The constraints on the reliability of this kind of vehicle impose relatively simple architecture for linking between the body and the ground. The number of degrees of freedom has to be sufficiently reduced to combine swiftness and the capacity of crossing large obstacles. Therefore, the choice of a joint between the drive line and the linking between the body and the ground has been discarded in this study.

Two drive line concepts are considered: wheel axle drive lines, and two-wheel bogie drive lines. The curves of Figure 1 show the trajectory of the connection between the suspension and the drive line during the clearance of two types of normalized obstacles. In this case, the geometry of the wheels is assumed to be unvariable and these obstacles have been chosen because they subject the suspensions to great effort. The maximum slope observed on the trajectory is reduced by half with the two-wheel bogie drive line when $L_1 = L_2$. Therefore, this concept allowed a smoother ground profile and consequently the excitations transmitted to the suspensions are reduced.

The model chosen of a quarter of a bogie vehicle is presented in Figure 2. It is a three-degree-of-freedom-system which takes the mass of the body and the mass and the inertia of the bogie into account. The passive combinations of the

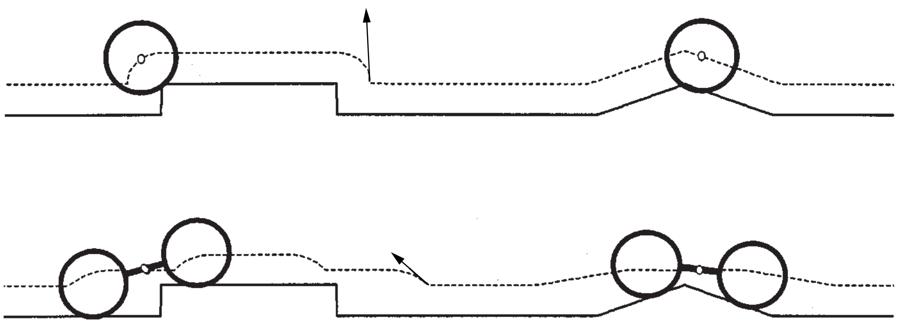

Figure 1. Axle trajectory for a wheel and a two-wheel bogie (δ_E).

suspension and the tires are modelled as a parallel combination of a spring and a viscous damper. If the wheels do not take off when crossing obstacles, the following equations can be written (a list of nomenclature is given in the Appendix):

$$\delta_{B1} = \delta_B + L_1\theta_B, \quad \delta_{B2} = \delta_B - L_2\theta_B. \tag{1}$$

The equations of the dynamics are

$$\begin{aligned} M_V\ddot{\delta}_V &= K_V(\delta_B - \delta_V) + C_V(\dot{\delta}_B - \delta_V) - M_V g, \\ m_B\ddot{\delta}_B &= K_V(\delta_V - \delta_B) + C_V(\dot{\delta}_V - \dot{\delta}_B) - m_B g \\ &\quad + K_{W1}(\delta_{E1} - \delta_B - L_1\theta_B) + C_{W1}(\dot{\delta}_{E1} - \dot{\delta}_B - L_1\dot{\theta}_B) \\ &\quad + K_{W2}(\delta_{E2} - \delta_B + L_2\theta_B) + C_{W2}(\dot{\delta}_{E2} - \dot{\delta}_B + L_2\dot{\theta}_B), \\ I_B\ddot{\theta}_B &= -\, C_B\dot{\theta}_B + [K_{W1}(\delta_{E1} - \delta_B - L_1\theta_B) + C_{W1}(\dot{\delta}_{E1} - \dot{\delta}_B - L_1\dot{\theta}_B)]L_1 \\ &\quad - [K_{W2}(\delta_{E2} - \delta_B + L_2\theta_B) + C_{W2}(\dot{\delta}_{E2} - \dot{\delta}_B + L_2\dot{\theta}_B)]L_2. \end{aligned} \tag{2}$$

By choosing a state vector $\mathbf{x}$ in such a way that the state variables coincide as far as possible with the measurements,

$$\mathbf{x} = {}^{\mathrm{t}}\{(\dot{\delta}_V) \quad (\dot{\delta}_B - \dot{\delta}_V) \quad (\dot{\theta}_B) \quad (\delta_B - \delta_V) \quad (\delta_{B1} - \delta_{E1} \quad (\delta_{B2} - \delta_{E2})\}, \tag{3}$$

the equations of the mechanical system subjected to the disturbances created during translation of the vehicle over the ground outline should be written in the form

$$\dot{\mathbf{x}} = \mathbf{A}_c\mathbf{x} + \mathbf{P}_c\mathbf{w} \tag{4}$$

with

$$
\mathbf{A}_c = \begin{bmatrix}
0 & \left(\dfrac{C_V}{M_V}\right) & 0 & \left(\dfrac{K_V}{M_V}\right) & 0 & 0 \\
-\left(\dfrac{C_{W1}+C_{W2}}{m_B}\right) & -\left(\dfrac{C_{W1}+C_{W2}}{m_B}\right) - C_V\left(\dfrac{1}{M_V}+\dfrac{1}{m_B}\right) & \dfrac{-1}{m_B}(C_{W1}L1 - C_{W2}L_2) & \left(-K_V\left(\dfrac{1}{M_V}+\dfrac{1}{m_B}\right)\right) & \left(-\dfrac{K_{W1}}{m_B}\right) & \left(-\dfrac{K_{W2}}{m_B}\right) \\
\dfrac{C_{W2}L_2 - C_{W1}L_1}{I_B} & \dfrac{C_{W2}L_2 - C_{W1}L_1}{I_B} & -\left(\dfrac{C_B + C_{W1}L_1^2 + C_{W2}L_2^2}{I}\right) & \left(\dfrac{C_B}{I_B}\right) & \left(-\dfrac{K_{W1}}{I_B}L_1\right) & \left(\dfrac{K_{W2}}{I_B}L_2\right) \\
0 & 1 & 0 & 0 & 0 & 0 \\
1 & 1 & (L_1) & 0 & 0 & 0 \\
1 & 1 & (-L_2) & 0 & 0 & 0
\end{bmatrix}, \qquad (5)
$$

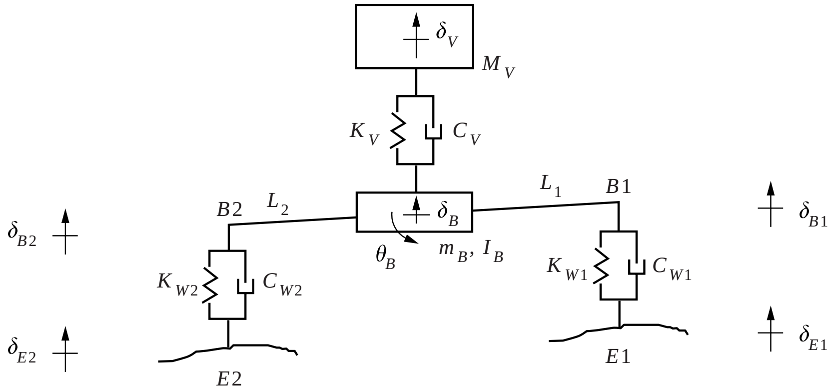

Figure 2. Modelling of a quarter vehicle equipped by a two-wheel bogie and a passive suspension.

$$\mathbf{P}_c = \begin{bmatrix} 0 & 0 & (-1) \\ \left(\dfrac{C_{W1}}{m_B}\right) & \left(\dfrac{C_{W2}}{m_B}\right) & 0 \\ \left(\dfrac{C_{W1}L_1}{I_B}\right) & \left(-\dfrac{C_{W2}L_2}{I_B}\right) & 0 \\ 0 & 0 & 0 \\ (-1) & 0 & 0 \\ 0 & (-1) & 0 \end{bmatrix} \quad \text{and} \quad \mathbf{w}(t) = \begin{Bmatrix} \dot{\delta}_{E1}(t) \\ \dot{\delta}_{E2}(t) \\ g \end{Bmatrix}, \tag{6}$$

and the initial conditions

$$\begin{aligned} (\delta_B - \delta_V)_0 &= \frac{M_V g}{K_V}, & (\dot{\delta}_B)_0 = (\dot{\delta}_V)_0 = 0, \\ (\delta_{E1} - \delta_{B1})_0 &= \frac{(M_V + m_B)g}{K_{W1}} \frac{L_2}{(L_1 + L_2)}, & (\dot{\delta}_{E1})_0 = (\dot{\delta}_{B1})_0 = 0, \\ (\delta_{E2} - \delta_{B2})_0 &= \frac{(M_V + m_B)g}{K_{W2}} \frac{L_1}{(L_1 + L_2)}, & (\dot{\delta}_{E2})_0 = (\dot{\delta}_{B2})_0 = 0. \end{aligned} \tag{7}$$

In the simulations, wheel take off is taken into account by cancelling all the values of the characteristics of the tires at this moment. The wheel takes off when the static deflection of the suspension is over-compensated. The simulations of Figure 3 are done on MATLAB® and SIMULINK® by using the optimized characteristics, given in Table 1, of a light military off-highway wheeled vehicle with passive suspensions. They show that the level of the acceleration of the body exceeds the limits of the expected performances when the speed of translation of the vehicle is 17 m/s and the obstacle has a step form. In this case the acceleration exceeds 25 m/s^2. Therefore, the actuation of the suspension is necessary.

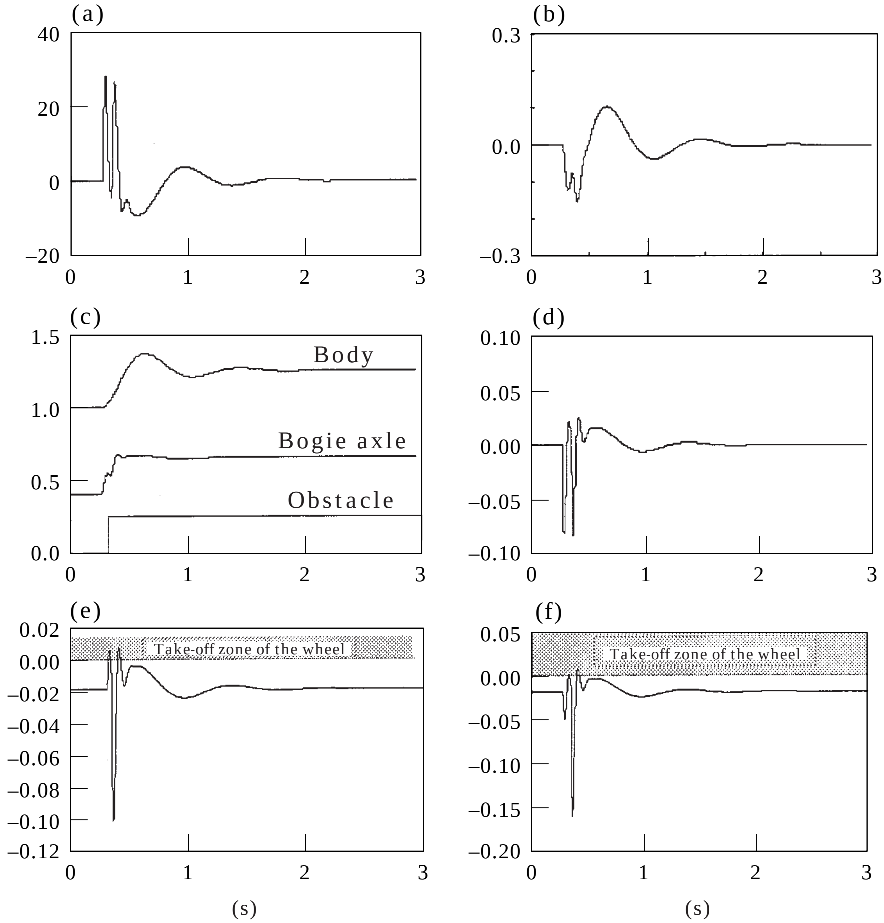

Figure 3. Dynamic behavior of a quarter vehicle with a two-wheel bogie and a passive suspension during a clearance of a step obstacle of 0·25 m with a 17 m/s (35 miles per hour) speed. (a) Body acceleration (m/s^2); (b) passive suspension deflection (m); (c) displacements (m); (d) relative displacement of bogie axle (m); (e) wheel 1 tire deflection (m); (f) wheel 2 tire deflection (m).

3. CONTROL STRATEGY

The control of suspension energy is supplied from the available energy of the vehicle. Thus, this part of consumption must be limited so as not to impede the vehicle's performance. For this purpose, active–passive controls are chosen in this study. Parallel and in-series designs are possible and described in Figure 4. Parallel design particularly reduces low magnitude vibrations in the high frequency range. In this case, instabilities occur more readily and the magnitude of clearance modifications between the ground and the body is limited. On the other hand the suspension fails if one of the hydraulic cylinders is locked. The in-series design is composed successively of a passive suspension, which reduces the disturbances, and an active part of which the action field is situated in the low frequencies. Thus, the cost of the components and the energy consumption

TABLE 1

Mechanical characteristics of the quarter real vehicle

Data	Numerical values	Designation
M_V	5·000 e + 02 kg	Mass of body of quarter vehicle
K_V	3·600 e + 04 N/m	Stiffness of passive suspension
C_V	2·900 e + 0.3 N s/m	Viscous damping coefficient of the passive suspension
m_B	7·00 e + 01 kg	Mass of bogie
I_B	8·000 e + 00 kg m^2	Inertia of bogie
K_{Wi}	1·500 e + 0.5 N/m	Stiffness of tires of the two wheels of the bogie
C_{Wi}	7·000 e + 02 N s/m	Viscous damping coefficient of tires of the two wheels of the bogie
C_B	1·000 e + 03 N s/rd	Viscous damping coefficient of the bogie
L_B	1·200 e + 00 m	Axle base of the two wheels of the bogie
R_{wi}	3·500 e–01 m	Radius of the two wheels of the bogie
m_W	7·000 e + 01 kg	Mass of equivalent wheel of the two-wheel bogie
K_W	3·000 e + 05 N/m	Stiffness of the tire of the equivalent wheel of the two-wheel bogie
C_W	1·400 e + 03 N s/m	Viscous damping coefficient of the equivalent wheel of the two-wheel bogie

are limited. Moreover, series design allows control of ground clearance over large obstacles.

The purpose of the control under study is to regulate the pitch, the roll and the ground clearance of the vehicle body. The control acts on the corresponding degrees of freedom through the active part of the suspension, which makes use of hydraulic assemblies mainly composed of a hydraulic cylinder and a servo valve. A standard control (see Figure 5) must take into account not only the dynamics of the mechanical part of the system but also the servo valves and hydraulic cylinders, the passive suspension, and the tire dynamics as well as managing the possible take-off of the bogie wheels. Consequently the design and the tuning are very intricate.

The hierarchical control strategy proposed in Figure 6 reduces the complexity of the control by dividing the management of the vehicle dynamics into two levels. A central controller takes into account the degrees of freedom linked to the pitch, the roll and the ground clearance of the vehicle body and delivers orders to local independent controllers devoted to each active suspension and bogie assembly. This solution can be carried out if the performances of the local controllers render transparent the ground linking dynamics to the central controller. The loop tuning of the control assembly is greatly reduced since the loop tuning of each controller can be carried out independently.

The study of the feasibility of this control strategy can be validated by a quarter vehicle, because the controllers are independent. In this case, the vertical displacement of the vehicle body is taken into account, thus the pitch adjustment is an extrapolation of the previous study.

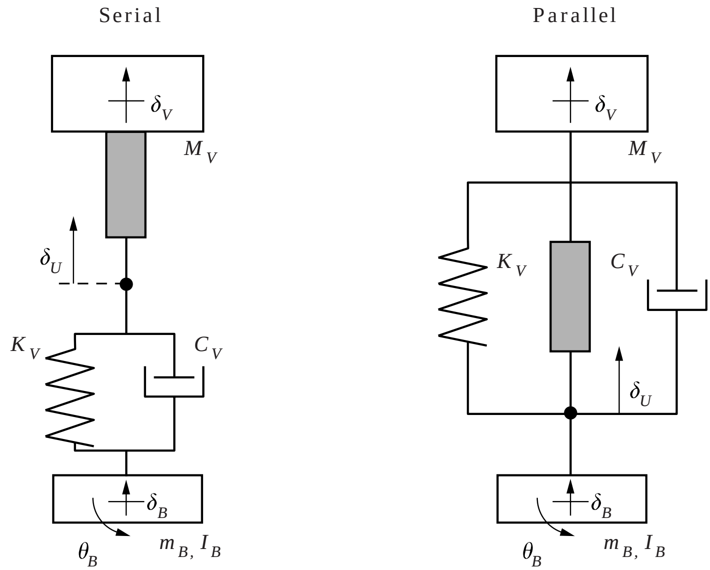

Figure 4. Active–passive suspension design.

4. DYNAMIC BEHAVIOR OF A QUARTER VEHICLE: THEORETICAL VIEW

4.1. LOCAL CONTROL

The quarter vehicle with active–passive suspension under study is composed of the previous passive components, a hydraulic cylinder driven by a servo valve and a two-wheel bogie. All these elements are mounted in series, as shown on Figures 4 and 7. The four-way double-stage servo valve used is modelled by the following linear equations [26]:

$$Q_L = k_q X_{tir} - k_c \Delta P_L, \tag{8}$$

$$Q_L/u_{SV} = k_t k_q R_{SV}/\{1 + (2\zeta_{SV}/\omega_{SV})s + (1/\omega_{SV}^2)s^2\}, \tag{9}$$

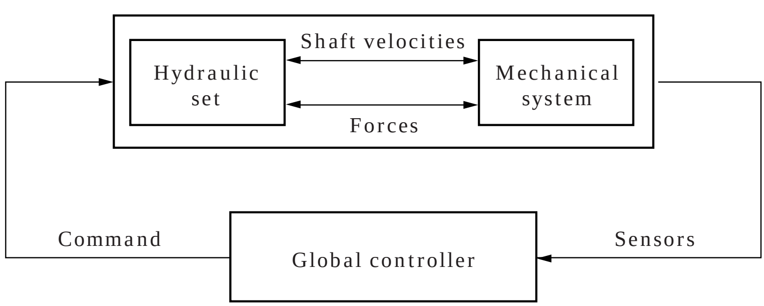

Figure 5. Standard control.

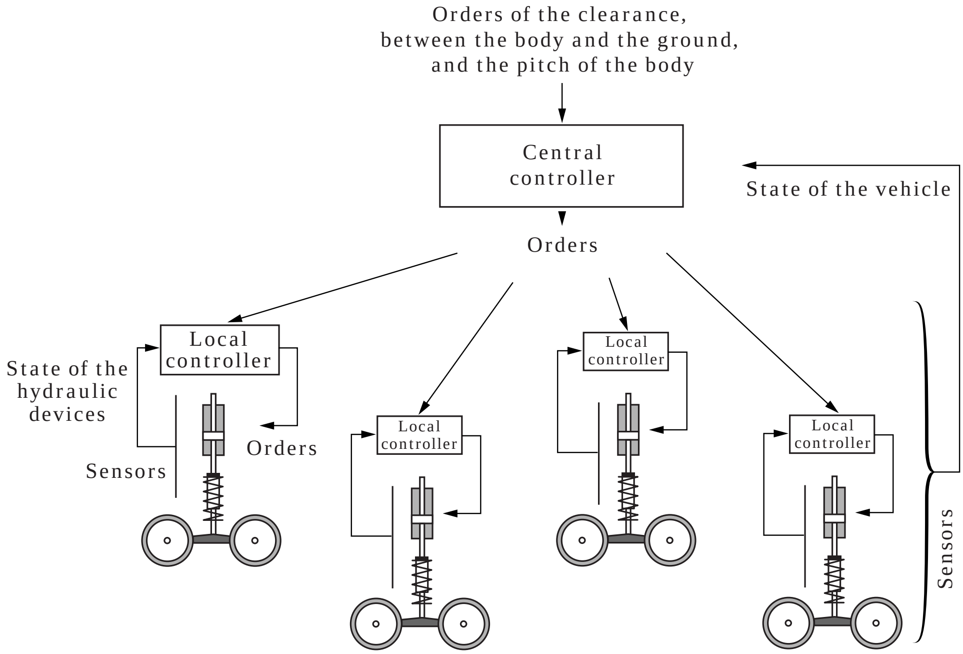

Figure 6. Two-level hierarchical control.

and the hydraulic cylinder presented in Figure 7 by the equations

$$Q_L = A_V \frac{\mathrm{d}X_V}{\mathrm{d}t} + C_{tp} \Delta P_L + \frac{V_0}{2B_e} \frac{\mathrm{d}\Delta PL}{\mathrm{d}t} \quad Q_L \cong A_V \frac{\mathrm{d}X_V}{\mathrm{d}t} + \frac{V_0}{2B_e} \frac{\mathrm{d}\Delta P_L}{\mathrm{d}t}, \tag{10, 11}$$

with:

$$X_V = \delta_V - \delta_U. \tag{12}$$

The dynamic equations of the body of the quarter vehicle and the shaft of the hydraulic cylinder are written as

$$M_V \ddot{\delta}_V = A_V \Delta P_L - f_V \frac{\mathrm{d}X_V}{\mathrm{d}t} - M_V g, \tag{13}$$

$$m_t \ddot{\delta}_U = -A_V \Delta P_L + f_V \frac{\mathrm{d}X_V}{\mathrm{d}t} + K_V(\delta_B - \delta_U) + C_V(\dot{\delta}_B - \dot{\delta}_U) - m_t g \tag{14}$$

and should be put in the form

$$\ddot{X}_V \frac{M_V m_t}{M_V + m_t} = A_V \Delta P_L - f_V \dot{X}_V - \frac{M_V}{M_V + m_t} [K_V(\delta_B - \delta_U) + C_V(\dot{\delta}_B - \dot{\delta}_U)]. \tag{15}$$

The local controller was regulated automatically as a function of speed. This system was developed in the continuation of this study. It must be fast enough

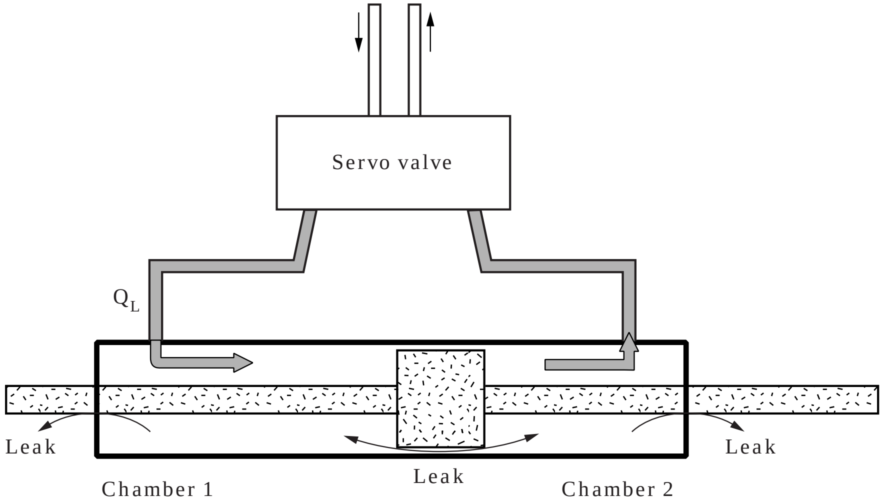

Figure 7. Design of the symmetric hydraulic set.

to ensure good compliance with the hierarchical control and allows neglecting the terms relative to the passive suspension in equation (15).

In addition, as the poles of the servo-valve are located far from the system working frequency range, they can also be neglected. The transfer function between the speed of the shaft and the tension of the servo-valve command is expressed by

$$\frac{\dot{X}_V}{u_{SV}} \approx \frac{k_t k_q R_{SV}}{A_V\left(1 + \dfrac{f_V V_0}{2B_c A_V^2} s + \dfrac{M_V m_t}{M_V + m_t} \dfrac{V_0}{2B_e A_V^2} s^2\right)}. \tag{16}$$

The control used is a P.I.D. type and the command must be written as

$$u_{SV} = K_{L/P} e + K_{L/I} \int_0^t e(\tau)\,\mathrm{d}\tau + K_{L/D} \frac{\mathrm{d}e}{\mathrm{d}t}, \tag{17}$$

with

$$e = (\dot{X}_{ORD} - \dot{X}_V). \tag{18}$$

4.2. CENTRAL CONTROL

The orders $\dot{X}_{ORD}$ are generated by the central controller located in the control loop presented in Figure 8. It is set up on the basis of an equivalent structural model described in equations (1) and (2) and shown in Figure 9. This unidirectional type model takes into account only the vertical displacements of the quarter vehicle. In this case, the effect of the rotation inertia of the bogie is not taken into account in this model; however, the vertical displacement of the axle is used (see Figure 1).

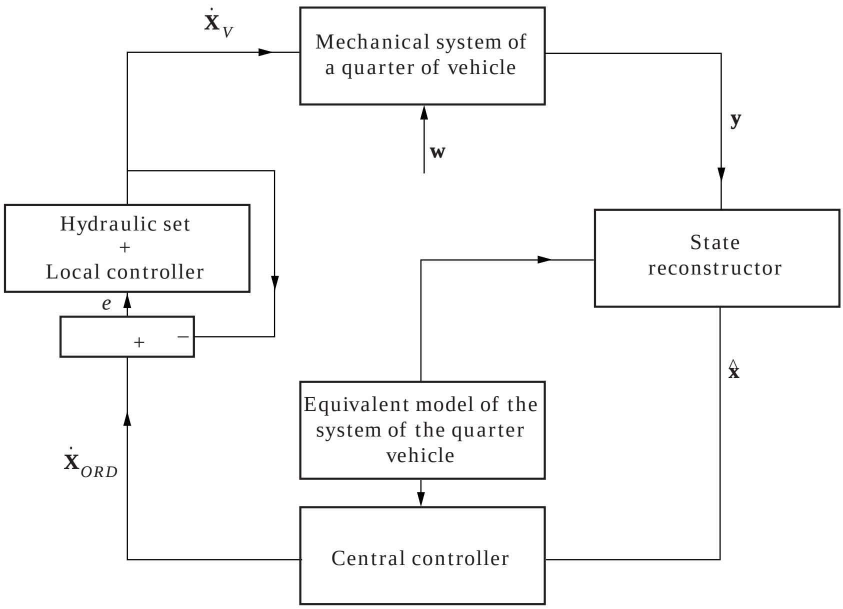

Figure 8. Block-diagram of a controlled quarter vehicle.

The corresponding equations can be written as

$$\dot{\mathbf{x}} = \mathbf{A}_c\mathbf{x} + \mathbf{B}_c\mathbf{u} + \mathbf{P}_c\mathbf{w} \tag{19}$$

with the following state and perturbation vector,

$$\mathbf{x} = {}^{\mathrm{t}}\{(\dot{\delta}_V) \quad (\dot{\delta}_B - \dot{\delta}_V) \quad (\delta_B - \delta_U) \quad (\delta_E - \delta_B)\}, \quad \mathbf{w} = \begin{Bmatrix} \dot{\delta}_E \\ g \end{Bmatrix}, \quad \mathbf{u} = \dot{\mathbf{X}}_V, \tag{20}$$

the matrices

$$\mathbf{A}_c = \begin{bmatrix} 0 & \left(\dfrac{C_V}{M_V}\right) & \left(\dfrac{K_V}{M_V}\right) & 0 \\ \left(-\dfrac{C_W}{m_B}\right) & \left[-\left(\dfrac{C_W}{m_B}\right) - C_V\left(\dfrac{1}{M_V} + \dfrac{1}{m_B}\right)\right] & \left[-K_V\left(\dfrac{1}{M_V} + \dfrac{1}{m_B}\right)\right] & \left(\dfrac{K_W}{m_B}\right) \\ 0 & 1 & 0 & 0 \\ -1 & -1 & 0 & 0 \end{bmatrix}, \tag{21}$$

$$\mathbf{B}_C = \begin{bmatrix} \left(\dfrac{C_V}{M_V}\right) \\ \left(-C_V\left(\dfrac{1}{M_V} + \dfrac{1}{m_B}\right)\right) \\ 1 \\ 0 \end{bmatrix}, \quad \mathbf{P}_c = \begin{bmatrix} 0 & -1 \\ \left(\dfrac{C_W}{m_B}\right) & 0 \\ 0 & 0 \\ 1 & 0 \end{bmatrix}, \tag{22}$$

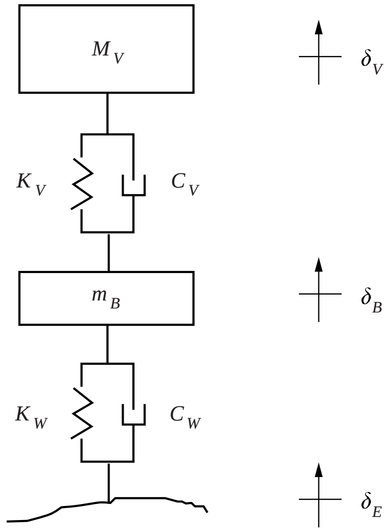

Figure 9. Equivalent model of a quarter vehicle.

and the following initial conditions:

$$\mathbf{x}_0 = {}^{\mathrm{t}}\{(0) \quad (0) \quad ((M_V g)/K_V) \quad ((M_V + m_B)g/K_W)\}. \tag{23}$$

The selected central controller uses a Linear Quadratic Gaussian algorithm (L.Q.G.), from state (20), which is matched with the specific purposes of the control [23, 27]. This algorithm requires a reconstruction of the state from the measurements and the command of the system. The control needs the addition of an extra state variable to remove the static errors described by

$$x_5 = z - (\delta_B - \delta_V). \tag{24}$$

Thus the equations can be written in the form

$$\dot{\mathbf{x}} = \left[\begin{array}{cccc:c} \multicolumn{4}{c:}{\mathbf{A}_c} & [0] \\ \hdashline 0 & -1 & 0 & 0 & 0 \end{array}\right]\mathbf{x} + \left[\begin{array}{c} \mathbf{B}_c \\ \hdashline 0 \end{array}\right]\dot{\mathbf{X}}_V + \left[\begin{array}{c:c} \mathbf{P}_c & [0] \\ \hdashline [0] & +1 \end{array}\right]\left\{\begin{array}{c} \mathbf{w} \\ \hdashline \mathrm{d}z/\mathrm{d}t \end{array}\right\}, \tag{25}$$

or as

$$\underline{\dot{\mathbf{x}}} = \underline{\mathbf{A}}_c\underline{\mathbf{x}} + \underline{\mathbf{B}}_c\dot{\mathbf{X}}_V + \underline{\mathbf{P}}_c\underline{\mathbf{w}}. \tag{26}$$

The selected performance criterion for the optimization is

$$J(\mathbf{x}, \mathbf{u}) = \frac{1}{2}\int_0^\infty \{\rho_1(\ddot{\delta}_V)^2 + \rho_2(\dot{\delta}_B - \dot{\delta}_V)^2 + \rho_3(\dot{X}_V)^2 + \rho_4(\delta_E - \delta_B)^2 + \rho_5(x_5)^2\}\,\mathrm{d}t, \tag{27}$$

in which ρ_1 expresses the objective of comfort, ρ_2 influences that of the clearance of the suspension in the system's frequency response, ρ_3 that of power consumption, ρ_4 that of road holding qualities, and ρ_5 which stabilizes the clearance between the body of the vehicle and the ground. This criterion can also be written in the form

$$J(\mathbf{x}, \mathbf{u}) = \frac{1}{2}\int_0^\infty \{{}^{\mathrm{t}}\mathbf{x}\,\mathbf{Q}\,\mathbf{x} + {}^{\mathrm{t}}\mathbf{u}\,\mathbf{R}\,\mathbf{u} + 2\,{}^{\mathrm{t}}\mathbf{u}\,\mathbf{N}\,\mathbf{x}\}\,\mathrm{d}t. \tag{28}$$

The weighting matrices **Q**, **R** and **N** depend on the selected purposes translated by the values of ρ_i. These values are chosen as a function of the control objectives which override comfort. They are determined by simulation.

The central controller is informed by the **x** state (20). However, the available measurements described by the output vector **y**,

$$\mathbf{y} = {}^{\mathrm{t}}\{(\ddot{\delta}_V)\;(\delta_B - \delta_V)\}, \tag{29}$$

also written in the form

$$\mathbf{y} = \begin{bmatrix} 0 & \dfrac{C_V}{M_V} & \dfrac{K_V}{M_V} & 0 \\ 0 & 0 & 1 & 0 \end{bmatrix}\mathbf{x} + \begin{bmatrix} \dfrac{C_V}{M_V} \\ 0 \end{bmatrix}\dot{\mathbf{X}}_V = \mathbf{Cx} + \mathbf{Du}, \tag{30}$$

show that not of all the state variables of equations (20) and (24) can be measured. Therefore, their reconstruction is necessary to inform the central controller. The L.Q.G. algorithm is well adapted to this job and makes use of a Kalman-Bucy observer [23]. It can be described by

$$\dot{\hat{\mathbf{x}}} = \mathbf{A}_c\hat{\mathbf{x}} + \mathbf{B}_c\mathbf{u} + \mathbf{L}(\mathbf{y} - \mathbf{C}\hat{\mathbf{x}}), \quad \mathbf{y} = \mathbf{C}\hat{\mathbf{x}} \tag{31}$$

It is included in the control loop as shown in Figure 10. The gain matrix **L** of the observer is optimized by the same algorithm as that used for the control. **L** can be written as

$$\mathbf{L} = -[{}^{\mathrm{t}}\mathbf{S}\,{}^{\mathrm{t}}\mathbf{C}\,\mathbf{R}_{obs}^{-1}], \tag{32}$$

with **S** being deduced from the resolution of the stationary algebraic equation of Ricatti:

$$-{}^{\mathrm{t}}\mathbf{A}_c\mathbf{S} - \mathbf{S}\,{}^{\mathrm{t}}\mathbf{A}_c - \mathbf{Q}_{obs} + \mathbf{S}\,{}^{\mathrm{t}}\mathbf{C}\,\mathbf{R}_{obs}^{-1}\mathbf{C}\,\mathbf{S} = 0. \tag{33}$$

4.3. SIMULATION OF THE HIERARCHICAL CONTROL OF THE QUARTER VEHICLE

The simulation results shown in Figures 11 and 12 emphasized the effect of the weighting adjustments, **a** and **b** of the two matrices. Their main purpose is to improve the vibratory insulation of the body when crossing step form obstacle by using a hydraulic active suspension. The hydraulic device has classical properties. In this case, the reduction of the magnitude of body acceleration is better than 20% for (a) the simulation and 50% for (b) the simulation in comparison to the quarter vehicle equipped with passive suspension. These improvements are obtained to the detriment of road holding qualities. If $\boldsymbol{\rho}_4$ is preponderant in relation to the other parameters, the criterion is more sensitive

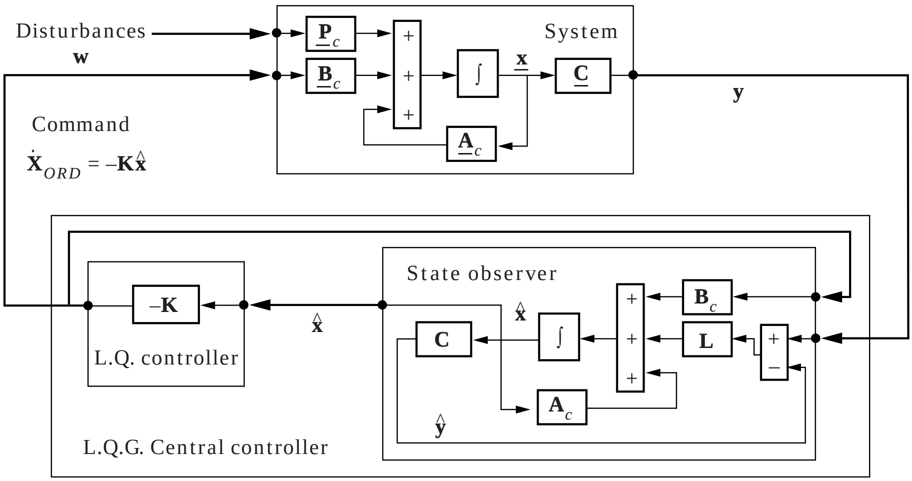

Figure 10. Principle of L.Q.G. central controller.

to the crushing of the tire and the control acts more specifically on the road holding qualities.

The control weighting and gain matrices for adjustment are the following:

$$\mathbf{Q} = \begin{bmatrix} 0 & 0 & 0 & 0 & 0 \\ 0 & 1{\cdot}69\times 10^4 & 2{\cdot}09\times 10^5 & 0 & 0 \\ 0 & 2{\cdot}09\times 10^5 & 2{\cdot}59\times 10^6 & 0 & 0 \\ 0 & 0 & 0 & 3{\cdot}1\times 10^4 & 0 \\ 0 & 0 & 0 & 0 & 5\times 10^4 \end{bmatrix},$$

$$R = 5{\cdot}02\times 10^6, \quad \mathbf{N} = [0 \quad 1{\cdot}68\times 10^4 \quad 2{\cdot}09\times 10^5 \quad 00],$$
$$\mathbf{K} = [0{\cdot}127 \quad 0{\cdot}233 \quad 5{\cdot}69 \quad 1{\cdot}95 \quad 1{\cdot}02].$$

For adjustment (b), the matrices become:

$$\mathbf{Q} = \begin{bmatrix} 0 & 0 & 0 & 0 & 0 \\ 0 & 2{\cdot}02\times 10^4 & 2{\cdot}51\times 10^5 & 0 & 0 \\ 0 & 2{\cdot}5\times 10^5 & 3{\cdot}11\times 10^6 & 0 & 0 \\ 0 & 0 & 0 & 7\times 10^3 & 0 \\ 0 & 0 & 0 & 0 & 2\times 10^4 \end{bmatrix},$$

$$R = 8{\cdot}02\times 10^6, \quad \mathbf{N} = [0 \quad 2{\cdot}02\times 10^4 \quad 2{\cdot}51\times 10^5 \quad 0 \quad 0]$$
$$\mathbf{K} = [0{\cdot}257 \quad 0{\cdot}559 \quad 9{\cdot}78 \quad 2{\cdot}02 \quad 0{\cdot}858].$$

The weighting and the gain matrices of the observer are

$$\mathbf{Q}_{obs} = {}^{t}\mathbf{B}_c \begin{bmatrix} 10^2 & 0 & 0 & 0 \\ 0 & 1 & 0 & 0 \\ 0 & 0 & 1 & 0 \\ 0 & 0 & 0 & 10^2 \end{bmatrix} \mathbf{B}_c, \quad \mathbf{R}_{obs} = \begin{bmatrix} 10^{-3} & 0 \\ 0 & 10^5 \end{bmatrix},$$

$$\mathbf{L} = \begin{bmatrix} -7{\cdot}43\times10^2 & 2{\cdot}25\times10^1 \\ 1{\cdot}34\times10^3 & -5{\cdot}35\times10^1 \\ 2{\cdot}25\times10^3 & 7{\cdot}43\times10^3 \\ 7{\cdot}37\times10^2 & 2{\cdot}22\times10^1 \end{bmatrix}.$$

As the working frequency bandwidths of the hydraulic device and the local controller are limited, the effect of the cut-off frequency can reduce performance of the entire system. Figure 13 and Table 2 show the influence of this cut-off frequency respectively on the acceleration of the body and the performances of the quarter vehicle. It can be noticed that the chosen hierarchical control is efficient with a cut-off frequency of the hydraulic devices higher than 30 Hz. These frequencies are those observed on classical hydraulic devices.

5. DYNAMIC BEHAVIOR OF A QUARTER OF A VEHICLE: EXPERIMENTAL ASPECT

5.1. DESCRIPTION OF THE TEST RIG

The experimental set-up shown in Figure 14 has been manufactured at the Direction Générale de l'Armement d'Angers, France, and installed at the Laboratoire de Mécanique des Structures de l'INSA de Lyon, France. It allows the simulation of crossing over large obstacles by a scale model of a quarter of a simplified off-highway vehicle. This experimental model has an approximate scale of 1/6. Its components have been chosen so that the static and dynamic behavior of the model are representative of a quarter of a real vehicle.

The characteristics of the test rig are given in Table 3; the process used to clear obstacles is achieved by blocking the horizontal displacement of a quarter vehicle when the profile of the ground is passing under it. It is composed of a quarter vehicle, a dynamic obstacle generator, a hydraulic unit, a welded steel frame and a device measurement and control system. The flow diagram of the test rig is shown in Figure 15.

The framework is made of welded girders the dimensions of which ensure great system rigidity.

The quarter vehicle can move only in the vertical direction. It includes a two-wheel bogie hinged on an axle. This axle, vertically guided by ball tubular casings, bears a passive type suspension. The upper part of this passive suspension is connected to the shaft of a double effect hydraulic cylinder. The body of the cylinder, the servo valve and the two oil pressure accumulators are

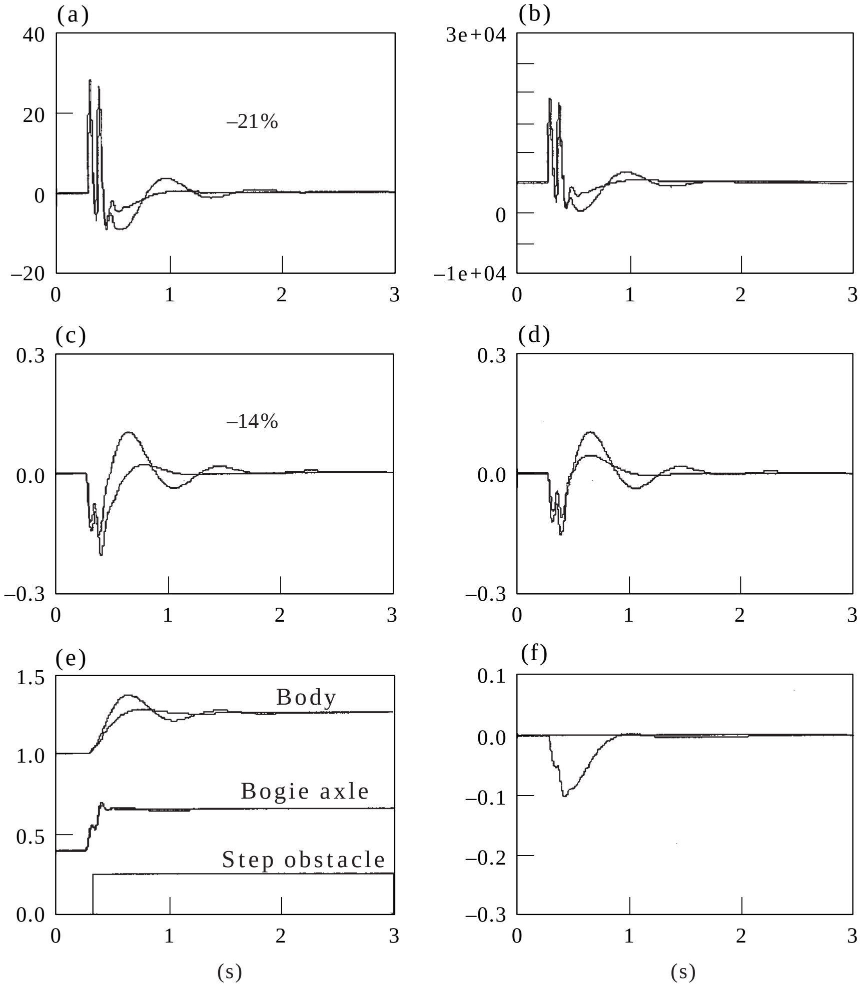

Figure 11. Dynamic behavior of the quarter vehicle equipped with a two-wheel bogie during the clearing of a 0·25 m step obstacle at a speed of 17 m/s. (a) Body acceleration (m/s^2); (b) produced force (N); (c) complete suspension deflection (M); (d) passive suspension deflection (M); (e) displacements (M); clearance of the shaft (M). (···, Passive suspension; —, velocity controlled active suspension, tuning (a).

mounted on a vertically guided trolley. These represent the mass of the quarter vehicle.

The dynamic obstacle generator simulates the profile of the ground with specific obstacles. These obstacles are mounted on the circumference of a large inertia disk, which is driven in rotation by a d.c. electric reduction-gear unit able to deliver high torque.

A hydraulic pump unit feeds the hydraulic set-up at high pressure, up to 250 bars.

The measurement and control devices include the following: two inductive picks-up for large displacements, which measure respectively the clearance of the axle of the hydraulic cylinder and that of the suspension; a capacitive accelerometer placed on the body of the hydraulic cylinder; a strain gage force

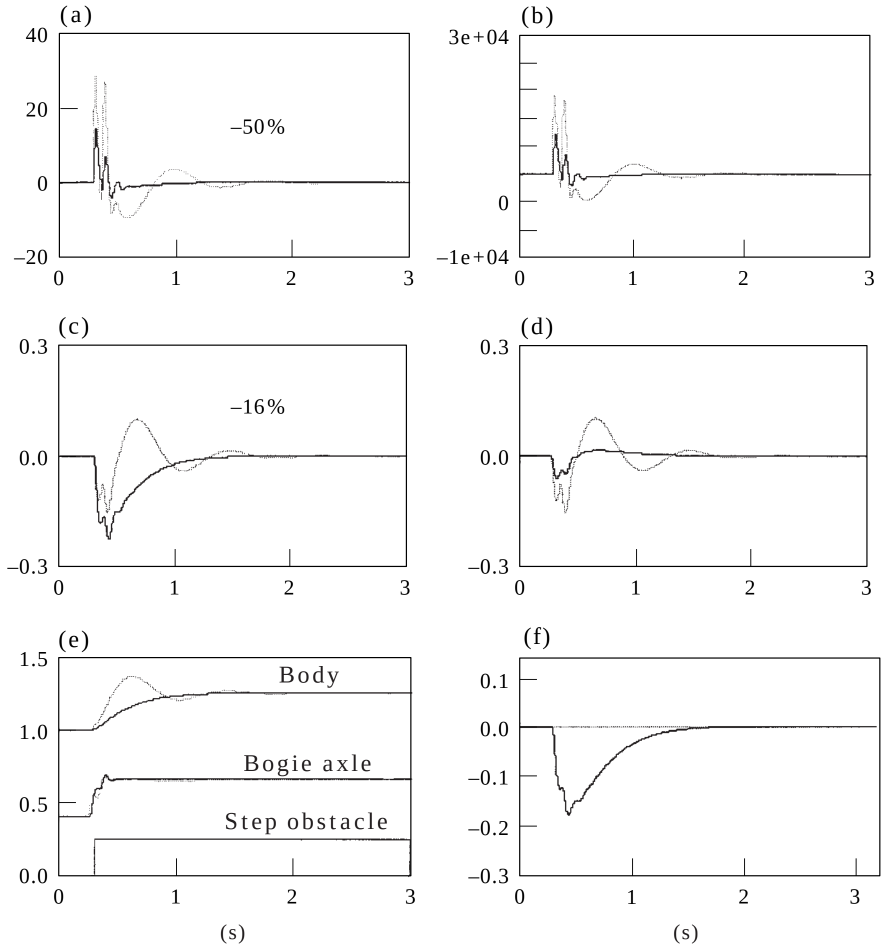

Figure 12. As Figure 11 but tuning (b).

transducer located between the axle of the hydraulic cylinder and the passive suspension; DSPACE cards are used such as the DS1003 card which is devoted to calculation and data processing management (numeric controller, supervision) and equipped with a DSP TMS320C40 processor; the DS2101 card, which informs the numeric controller, has five 12-bit analog-digital converters (A.D.C.) each with a conversion speed ratio of 3 μs; DS2002 card, which transmits the orders from the numeric controller to the actuator, has a 12-bit digital-analog converter (D.A.C.) with a conversion speed ratio of 5 μs; all these cards are located in a P.C. and have been implemented with MATLAB® and SIMULINK® environments; anti-aliasing filters are put on each measurement channel; their cut-off frequency is set of at 625 Hz.

5.2. SCALE MODEL PARAMETERS

The stiffness variation curves deduced from experiments, related to the pressure of the tire, can be approximated by straight lines and the results are given in Table 3.

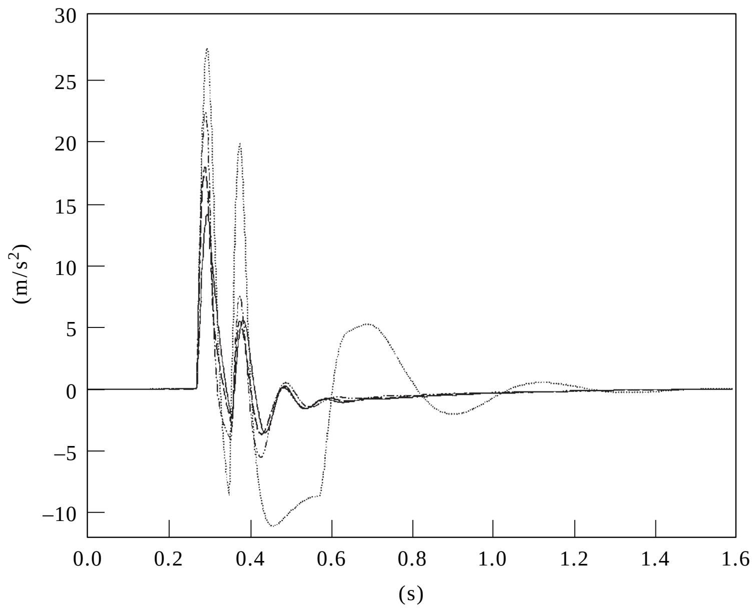

Figure 13. Comparison of the performances of the local control with different hydraulic sets for the acceleration of the body, during the clearing of a 0·25 m height at a speed of 17 m/s, —, Perfect, $F_c \to \infty$; - - -, F_c = 30 Hz; —·· — ··, F_c = 15 Hz; ······ F_c = 3 Hz, F_c = cut-off frequency of the local control.

The characteristics of the passive combination were reset based on the responses of the mechanical system when the shaft of the hydraulic cylinder was blocked and the scale model crossed over the obstacles. Two obstacles were used, half sine and trapezoidal, at three speeds of translation: 1, 1·5 and 2 m/s. For a trapezoidal obstacle and a speed of 1·5 m/s, the experimental and simulation results are shown in Figure 16. The good test reproducibility and the shapes of the curves, of both the experiments and the simulations, validate the model and the parameters given in Table 3 of the quarter vehicle with a passive suspension.

TABLE 2

Comparison of performances as a function of the cut-off frequency of the hydraulic device

	F_c = 3 Hz	F_c = 15 Hz	F_c = 30 Hz	$F_c \to \infty$
Acceleration of body of the quarter vehicle (m/s^2)	min. −11·2 max. 27·6	min. −5·6 max. 22·4	min. −3·69 max. 17·9	min. −3·61 max. 14·1
Displacement of body of the quarter vehicle (m)	0·277	0·28	0·28	0·281
Clearance of passive suspension (m)	min. −0·116 max.0·102	min. −0·084 max. 0·0123	min. −0·068 max. 0·012	min. −0·0619 max. 0·0129
Speed of the shaft of hydraulic cylinder (m/s)	min. −1·25 max. 1·05	min. −2·6 max. 0·68	min. −3·08 max. 0·656	min. −3·34 max 0·806
Force of hydraulic cylinder (N)	min. −683 max. 18690	min. 2108 max 16090	min. 3061 max. 13880	min. 3100 max. 11952

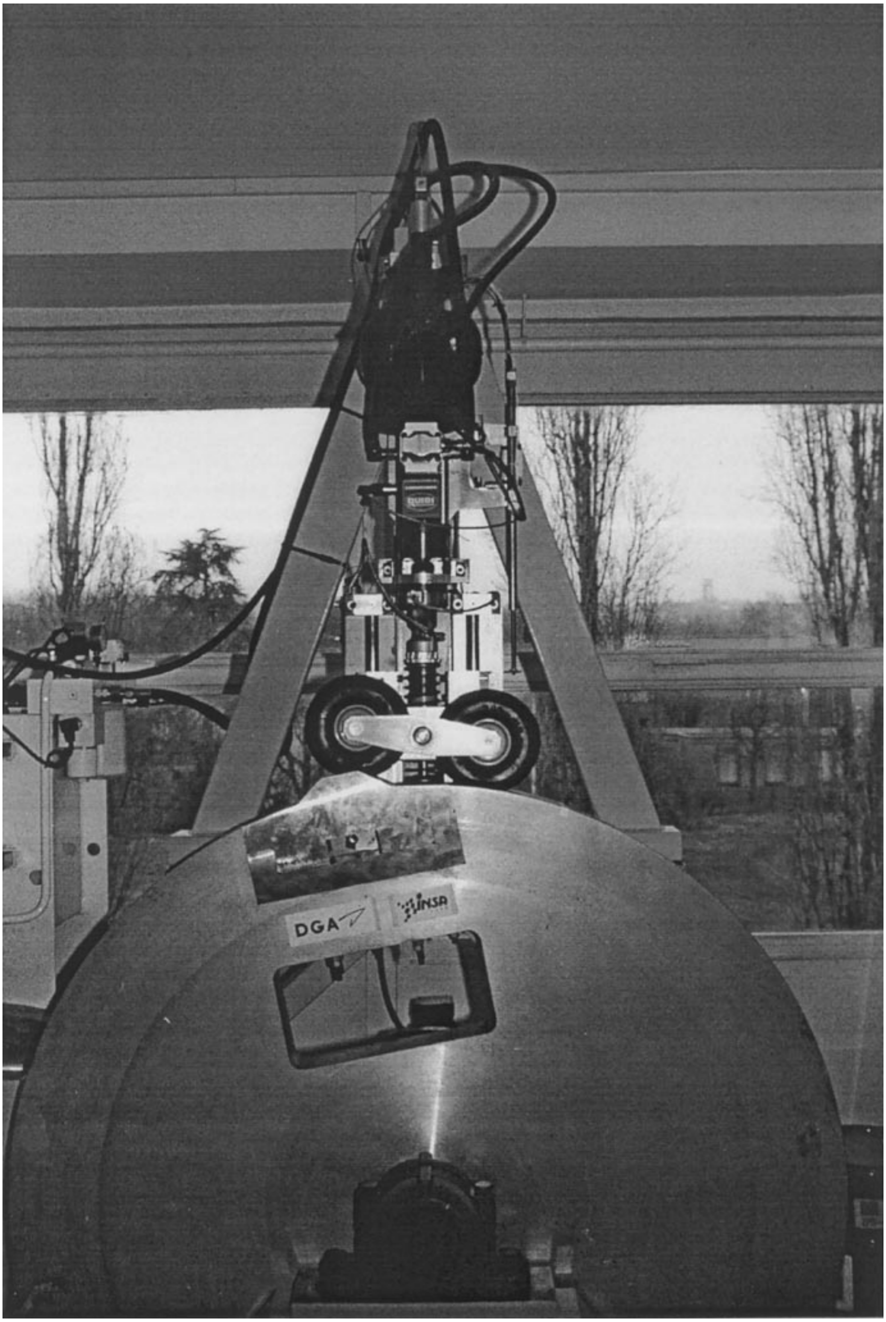

Figure 14. Experimental set-up.

The experimental data of the MOOG servo valve are provided by the manufacturer for a pressure of 210 bars and a differential pressure of 70 bars, between the two chambers of the hydraulic cylinder. The characteristics of the actuator were tuned by using a three-degree-of-freedom model. The cut-off frequency was located far higher than the working frequency range of the scale model.

TABLE 3
Technical specification of the test rig

Welded framework	Mass	800 kg
	Depth	2·20 m
	Width	1·70 m
	Height	3.20 m
Obstacle generator		
Cam wheel	Mass	500 kg
	Diameter	1·6 m
	Thickness	0·10 m
Trapezoidal obstacle	Large basis	0·18 m
	Small basis	0·07 m
	Height	0·04 m
Half-sinus obstacle	Length	0·15 m
	Height	0·04 m
Back-geared motor	Power	4 kW
	Maximum torque	1200 Nm
Motor-driven pump		
Pump	Power	4 kW
	Nominal output	8·4 l/mn
	Maximum pressure	250 bars
Hydraulic accumulator	Volume	$2{\cdot}5 \times 10^{-3}$ m^3
	Pressure	150 bars
High pressure hydraulic accumulator	Volume	$0{\cdot}7 \times 10^{-3}$ m^3
	Inflation pressure	200 bars
Low pressure hydraulic accumulator	Volume	$0{\cdot}7 \times 10^{-3}$ m^3
	Inflation pressure	3·4 bars
Scale model of quarter vehicle		
Body	Mass	45 kg
Bogie	Mass	9 kg
Wheel	Clearance between axle-wheel and ground	0·085 m
Servo valve	Nominal output	19 l/mn
Hydraulic cylinder symmetric double effect	Effective section	2×10^{-4} m^2
	Maximum force	4000 N
	Clearance of the shaft	0·20 m

5.3. EXPERIMENTS

A first experiment was carried out to compare the dynamic behavior of the quarter vehicle with a passive suspension, equipped successively with a wheel and with a two-wheel bogie. The results shown in Figure 17, were obtained for the clearance of a half sinus obstacle at a speed of 1·5 m/s. They proved that performances of the quarter vehicle with a two-wheel bogie were better at smoothing the ground profile. In this case, the reduction of the maximum acceleration magnitude of the body was 25%, while the clearance of the suspension and the force transmitted to the body were reduced respectively by 37 and 20%.

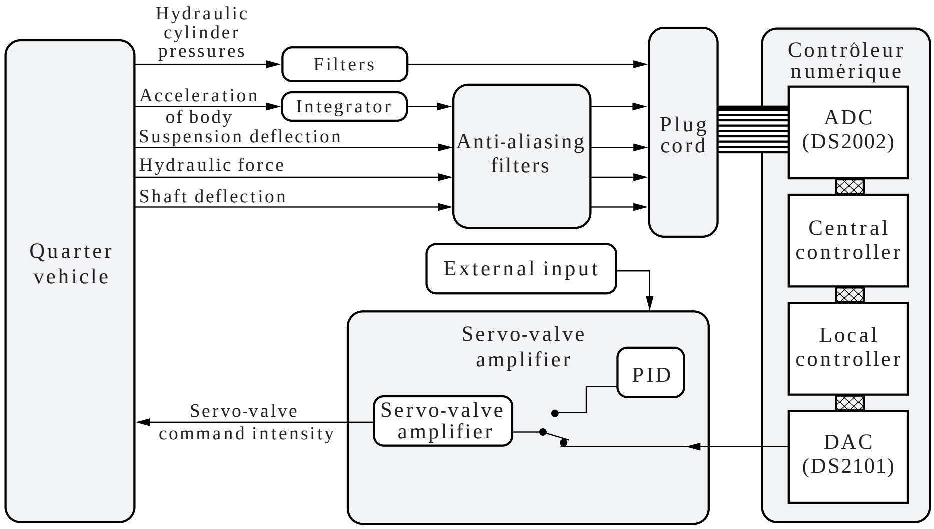

Figure 15. Flow diagram of control feedback.

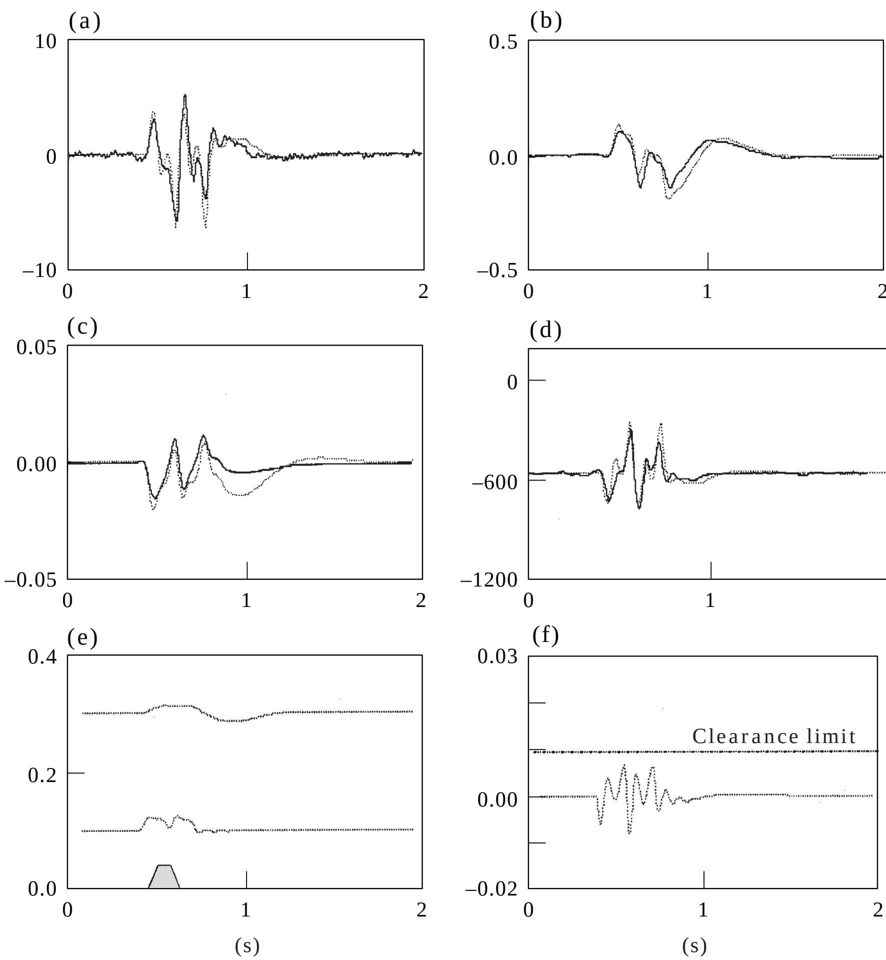

Figure 16. Dynamic behavior of a two-wheel bogie quarter vehicle with passive suspension during the clearance of a trapezoidal obstacle at a speed of 1·5 m/s. (—, Experimental data; ····, simulated results. (a) Body acceleration (m/s^2); (b) absolute velocity of the body (m/s); (c) complete deflection suspension; (d) force measured on shaft extremity (N); body displacement and the wheel (M); (f) time deflection (M).

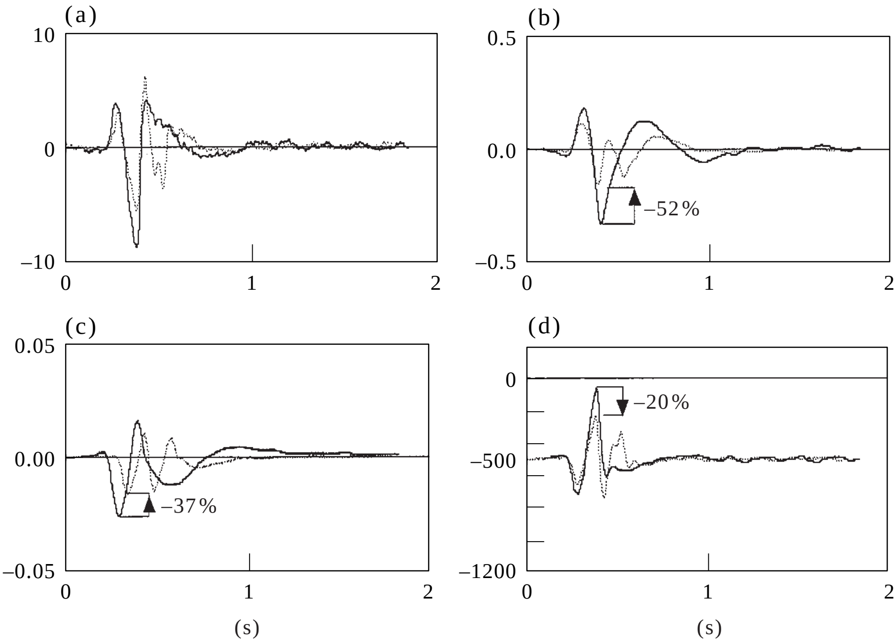

Figure 17. Experimental comparison between wheel and bogie for a half sine obstacle at a speed of 1·5 m/s. —, Passive wheel vehicle; ····, passive bogie vehicle. (a) Body acceleration (m/s^2); (b) absolute speed of body (m/s); (c) complete deflection suspension (M); (d) force measured on shaft (N).

The last experimental stage deals with the validation of the efficiency of the serial active–passive suspension of the scale model.

The whole device makes use of the hierarchical control described above. It includes not only the L.Q.G. algorithm and the P.I.D. control, but also specific signal processing to improve the signal to noise ratio.

The relative speed of the shaft in relation to the body of the hydraulic cylinder is obtained by derivation of the displacement signal measured by the internal L.V.D.T. transducer of the hydraulic cylinder. This signal is then processed by two numeric filters in series. The first is a low pass filter with a cut-off frequency of 40 Hz carried out by successive averaging of three samples. The second is a selective frequency notch filter which eliminated the electric interference due to the national network frequency (50 Hz) which appeared on the measured signals.

The vertical speed of the body was obtained by integration of the signal fed by a capacitive accelerometer mounted on the body of the vehicle. This signal was processed by a Butterworth high-pass filter of the sixth order in series with a one-pole low-pass filter. The cut-off frequency of the high-pass filter was set at 0·3 Hz to avoid the effect of the integration of the d.c. component supplied by the accelerometer. The low-pass filter with a cut-off frequency of 40 Hz, improved the signal to noise ratio in the range of the working frequencies.

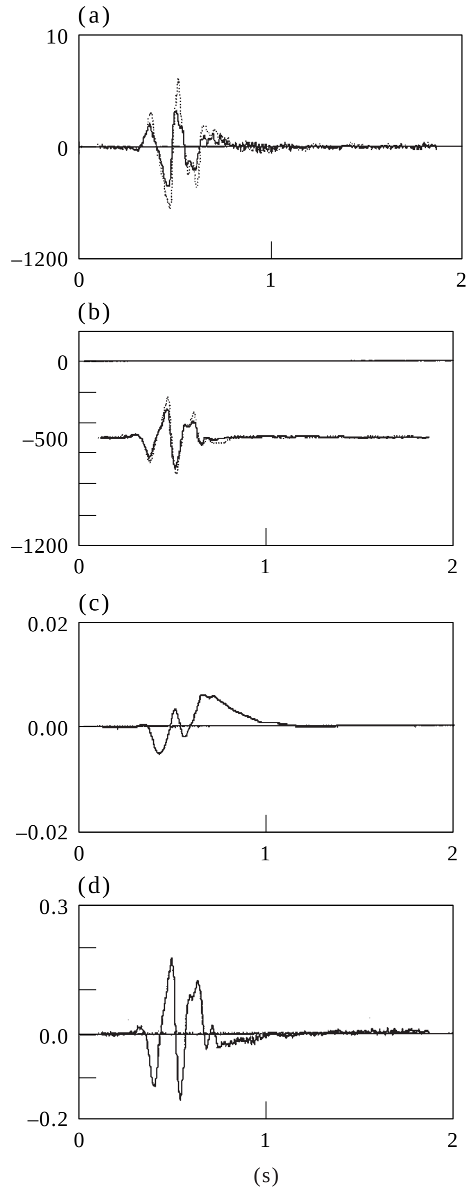

Figure 18. Comparison of the experimental results of the behavior of a two-wheel bogie quarter vehicle during the clearance of a half sine obstacle at a speed of 1·5 m/s ····, Passive suspension; —, active suspension. (a) Body acceleration (m/s^2); (b) force measured on shaft (N); (c) shaft deflection (M); (d) speed of shaft (m/s).

Figures 18 and 19 compare the dynamic behaviors of the quarter vehicle, equipped successively with passive suspension and serial active–passive suspension, during the crossing of half sinus and trapezoidal obstacles at a speed of 1·5 m/s. The improvement obtained in the case of a serial active–passive suspension and the clearing of the trapezoidal obstacle was about 40% for the

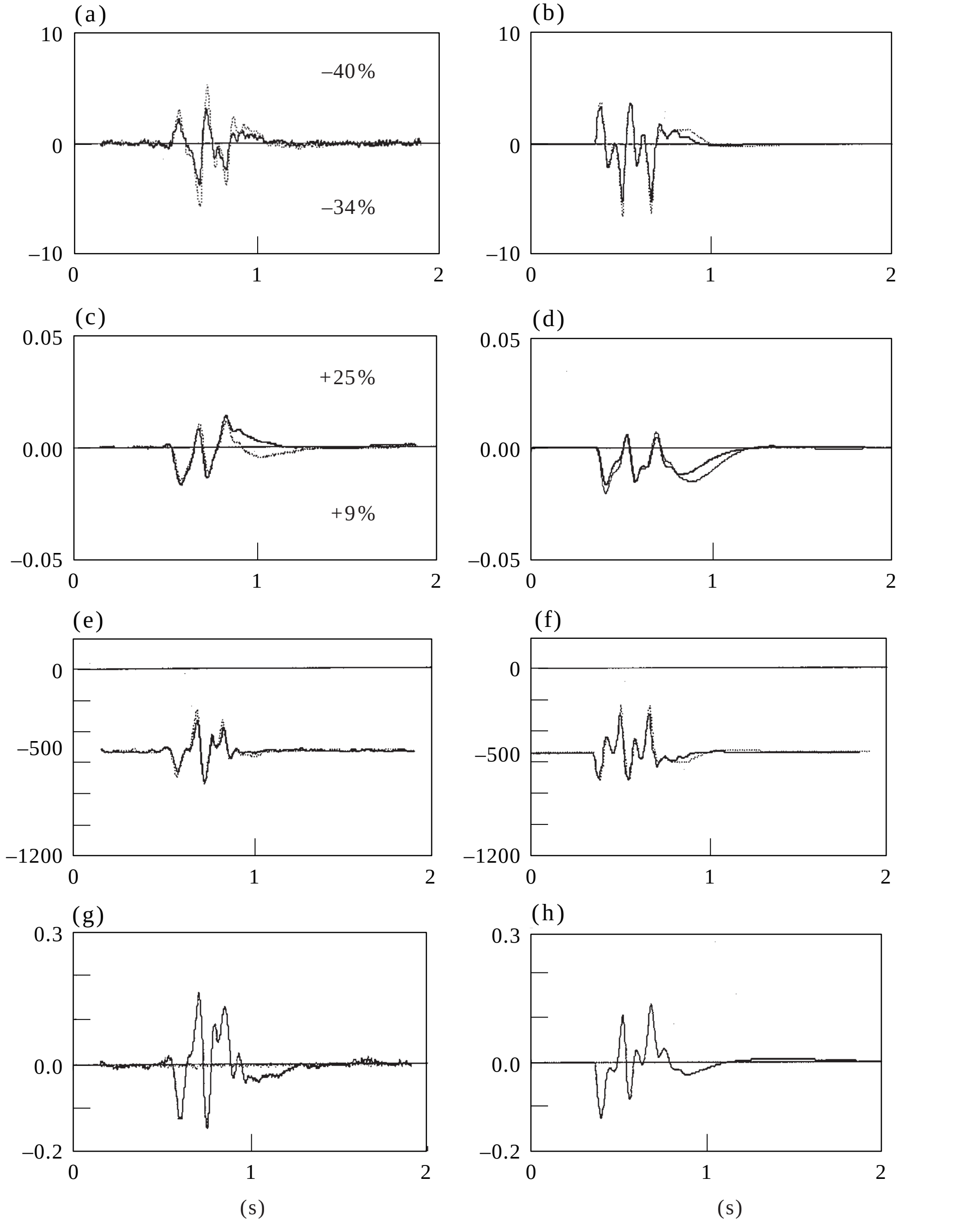

Figure 19. Comparison of the dynamic behavior of a two-wheel bogie quarter vehicle during the clearance of a trapezoidal obstacle at a speed of 1·5 m/s. ····, Passive suspension; —, active suspension. (a, b) Body acceleration (m/s^2); (c, d) complete deflection suspension (M); (e, f) force measured on shaft (N); (a, h) absolute speed of shaft (m/s).

maximum magnitude of the body acceleration. The other performances are presented in Figure 20 and obtained for three speeds of translation: 1, 1·5 and 2 m/s. for the extreme upper speeds, the results of the, tests showed a reduction of the performances. They are probably linked to the non-linear effects, not

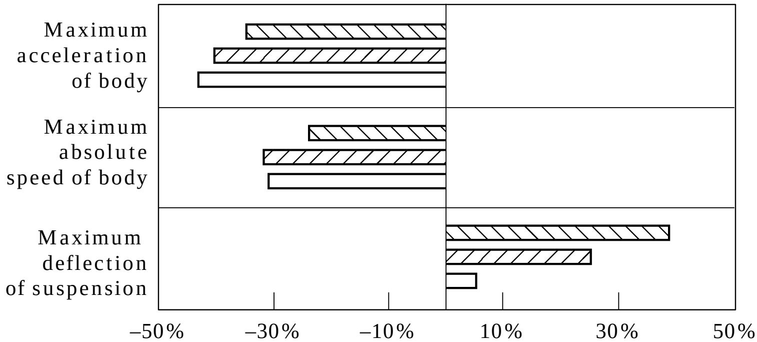

Figure 20. Characterization of active suspension performance in relation to the passive suspension of a two-wheel bogie quarter vehicle during the clearance of a trapezoidal obstacle. Vehicle velocity (m/s): ⧅, 20; ▨, 15; □, 10.

taken into account in this study, essentially induced by the hydraulic actuator and the limits of the device.

6. CONCLUSION

This study deals with a new concept of suspension and locomotion for an off-highway vehicle to permit the rapid crossing of large obstacles, and the modification of the clearance between the body and the ground.

Firstly, the geometric study of obstacle crossing led to choosing a two-wheel bogie drive line which improves performance by smoothing the profile of the ground. Then a dynamic study of the behavior of a quarter vehicle was carried out, leading to the selection of a hydraulic serial active–passive suspension requiring limited energy consumption and using classical technological components.

These suspensions were controlled by a two-level hierarchical controller which takes into account the clearance between the body and the ground, the pitch and the dynamics of the whole vehicle.

By using the characteristics of current light military off-highway vehicles, simulations were carried out, permitting optimization of the controller subjected to the technological constraints of the devices thereby improving the vibratory isolation of the body.

A scale model of a quarter vehicle was made to show the efficiency of the proposed concept of linkage between the body and the ground for crossing large standardized obstacles. After identifying the model parameters, tests were performed. The experimental results confirmed those of the simulations and showed improved capacities for crossing large obstacles at speed. The improvements made to vehicle performance by using this type of suspension can now be considered seriously.

ACKNOWLEDGMENTS

This paper reports work supported by D.G.A. (Direction Générale de l'Armement) E.T.A.S. Angers France, under contract. The authors would particularly like to express their thanks to Mr Renou and Mr Tamisier for their contributions.

REFERENCES

1. J. C. LARMINIE 1992 *I.S.T.V.S. Conference on Off-road Vehicles* 10–11 *June*, 90–111. The value of cross-country mobility.
2. B. T. FIJALKOWSKI 1990 *Proceedings of the* 10*th International Conference of the I.S.T.V.S., Kobe, Japan*, 20–24 *August* **3**, 783–797. Very advanced propulsion spheres for high speed tracked vehicles.
3. C. E. THORPE 1991 *International Journal of Pattern Recognition and Artificial Intelligence* **5**, 383–397. Mobile robots.
4. J. D. BURKE 1992 *Missions, technologie et conception de véhicules mobiles planétaires*, 45–60. CNES Toulouse: Cépadues Editions, ISBN 2-85428-331-7, Past US studies and developments for planetary rovers.
5. A. L. KEMURDJIAN *et al.* 1992 *Missions, technologie et conception de véhicules mobiles planétaires*, 25–43. CNES, Toulouse: Cépadues Editions, ISBN 2-85428-331-7. Soviet developments of planet rovers in period of 1964–1990.
6. S. HIROSE 1991 *Proceedings of* 5*th International Conference on Advanced Robotics, Pisa, Italy*, 19–22 *June* **1**, 12–17. Three basic types of locomotion in mobile robots.
7. R. S. SHARP and S. A. HASSAN 1984 *Society of Environmental Engineers Conference on Dynamics in Automotive Engineering, Cranfield, UK,* 5–6 *April*, 104–112. The fundamentals of passive automotive suspension system design.
8. R. M. GOODALL and W. KORTÜM 1983 *Review of the State-of-the-art and Future Potential Vehicle System Dynamics* **12**, 225–257. Active controls in ground transportation.
9. D. C. KARNOPP 1995 *Journal of Mechanical Design—*50*th Anniversary of the Design Engineering Division* **117**, 177–185. Active and semi-active vibration isolation.
10. M. TOMIZUKA and J. K. HEDRICK 1995 *Vehicle System Dynamics* **24**, 449–468. Advanced control methods for automotive applications.
11. J. K. HEDRICK and D. N. WORMLEY 1975 *State of the Art Review, Mechanics Transportation Suspension Systems, ASME Monograph, AMD* **15**. Active suspensions for ground transportation vehicles.
12. D. HROVAT and W. F. POWERS 1988 *IEEE Control Systems Magazine* **8**, 3–10. Computer control systems for automotive power trains.
13. E. M. ELBEHEREY, D. C. KARNOPP, M. E. ELARABY and A. M. ABDELRAAOUF 1995 *Classified Bibliography. Vehicle System Dynamics* **24**, 231–260. Advanced ground vehicle suspension systems.
14. T. IWAMOTO and H. YAMAMOTO 1990 *Journal of Mechanisms, Transmissions and Automation in Design* **112**, 289–294. Mechanical design of variable configuration tracked vehicle.
15. P. BOICHOT and L. JÉZÉQUEL 1996 *Mécanique Industrielle et Matériaux* **49**, 130–132. Etude expérimentale d'un amortisseur piloté.
16. I. YOUN and A. HAC 1995 *Journal of Sound and Vibration* **180**, 475–492. Semi-active suspensions with adaptive capability.
17. R. A. WILLIAMS 1992 *IEE Colloquium on Active Suspension Technology for Automotive and Railway Applications, Digest no* 1992–193, 2·1–2·4. Automotive active suspension.

18. M. DUVAL-DESTIN 1993 *Actes du Colloque sur la Mécanique et les Armements Aéroterrestres, Arcueil-France*, 256–268. La robotique mobile militaire: une opportunité pour l'evolution des véhicules de combat?
19. D. C. KARNOPP 1987 *Vehicle System Dynamics* **16**, 355–380. Active suspension based on fast load levelers.
20. M. M. ELMADANY 1990 *Vehicle System Dynamics* **19**, 19–47 Ride performance potential of active fast load leveling systems.
21. B. MAILLARD, J. DER HAGOPIAN and L. GAUDILLER 1996 *Mécanique Industrielle et Matériaux* **49**, 82–84. Une suspension hydraulique active–passive pour le franchissement rapide de grands obstacles.
22. E. K. BENDER, D. C. KARNOPP and I. PAUL 1967 *ASME Paper* 67-*Trans*-12. On the optimization of vehicle suspension using random process theory.
23. R. E. KALMAN and R. S. BUCY 1961 *ASME Transactions D, Journal of Basic Engineering* **83**, 95–108. New results in linear filtering and prediction theory.
24. C. YUE, T. BUTSUEN and J. K. HEDRICK 1988 *Proceedings of the American Control Conference, Atlanta*, 2373–2378. Alternative laws for automotive active suspensions.
25. E. M. ELBEHEREY, D. C., KARNOPP, M. E. ELARABY and A. M. ABDELRAAOUF 1996 *Vehicle System Dynamics* **26**, 197–222. Suboptimal control design of active and passive suspension based on a full car model.
26. H. E. MERRITT 1967 *Hydraulic Control Systems*. New York: John Wiley & Sons.
27. L. GAUDILLER and J. DER HAGOPIAN 1996 *Journal of Sound and Vibration* **193**, 713–741. Active control of flexible structures using a minimum number of components.

APPENDIX : NOMENCLATURE

$\mathbf{A}_c$	progression matrix of the quarter vehicle
$\underline{\mathbf{A}}_c$	increased progression matrix of the quarter vehicle
$\mathbf{A}_V$	cross-section of the hydraulic cylinder chamber
$\mathbf{B}_c$	translation matrix of the command of the quarter vehicle
$\underline{\mathbf{B}}_c$	increased translation matrix of the command of the quarter vehicle
B_e	effective modulus of compressibility of the hydraulic fluid
$\mathbf{C}$	matrix of the outputs
C_B	viscous damping coefficient of the bogie in rotation
C_{tp}	leakage coefficient
C_V	viscous damping coefficient of the passive suspension
C_W	viscous damping coefficient of the tire of the equivalent model
C_{Wi}	viscous damping coefficient of the tire of wheel i of the bogie
$\mathbf{D}$	matrix of the direct transmission
e	difference between the order and the output of the local controller
f_V	viscous damping coefficient.
g	gravitational acceleration
I_B	rotational inertia of the bogie at point B
k_c	flow rate/pressure coefficient of the servo valve
$K_{L/P}$	proportional gain of the local controller
k_q	flow rate gain of the servo valve
k_t	static gain of the first stage of amplification of the servo valve
$K_{L/I}$	integral gain of the local controller

$K_{L/D}$	derivative gain of the local controller
K_V	stiffness of the passive suspension
K_W	stiffness of the tire of the wheel model equivalent to the two-wheel bogie
K_{Wi}	stiffness of the tire of wheel i of the bogie
L_B	axle base of the bogie wheels
L_i	center distance of axes between the link of the bogie and the axle of wheel i
m_B	mass of the bogie, mass of the wheel model equivalent to the two-wheel bogie
m_t	mass of the shaft-piston of the hydraulic cylinder and the linking between the hydraulic cylinder shaft and the passive suspension assembly
M_V	mass of body of the quarter vehicle
$\mathbf{P}_c$	disturbance matrix of the quarter vehicle
$\underline{\mathbf{P}}_c$	increased disturbance matrix of the quarter vehicle
$\mathbf{Q}$, $\mathbf{R}$, $\mathbf{N}$	weighting matrices of the crossed quadratic criterion of the control
$\mathbf{Q}_{obs}$, $\mathbf{R}_{obs}$	weighting matrices of the quadratic criterion of the observer
Q_L	total servo valve flow rate
Q_{SV}	internal servo valve flow rate
R_{sv}	apparent servo valve resistance
R_{wi}	radius of bogie wheels
$\mathbf{S}$	Ricatti matrix of the observer
$\mathbf{u}$	control vector
u_{sv}	tension of servo valve command
u_{SV}	command of local controller
V_0	volume of hydraulic cylinder chambers when the piston is in central position
$\mathbf{w}$	disturbances vector
$\underline{\mathbf{w}}$	increased disturbances vector
$\mathbf{y}$	output vector of the quarter vehicle
$\mathbf{x}$,$\dot{\mathbf{x}}$	state vector and its derivative in relation to time
$\underline{\mathbf{x}}$,$\underline{\dot{\mathbf{x}}}$	increased state vector and its derivative in relation to time
$\hat{\mathbf{x}}$	vector of the estimate state
$\dot{\mathrm{X}}_{ORD}$	velocity order of the local controller
X_{tir}	displacement of servo valve distributor slide
X_V	relative displacement of shaft from the hydraulic cylinder body
$\hat{\mathbf{y}}$	vector of the estimate output
z	order of the clearance between the ground and the body of the quarter vehicle
δ_B,$\dot{\delta}_B$,$\ddot{\delta}_B$	vertical displacement, velocity and acceleration of the axle of the bogie
δ_{Bi},$\dot{\delta}_{Bi}$,$\ddot{\delta}_{\beta i}$	vertical displacement, velocity and acceleration of wheel i of the bogie
δ_{Ei},$\dot{\delta}_{Ei}$	assigned vertical displacement, velocity and acceleration of the contact point i tire ground

$\delta_U, \dot{\delta}_U, \ddot{\delta}_U$	vertical displacement, velocity and acceleration of the hydraulic cylinder shaft
$\delta_V, \dot{\delta}_V, \ddot{\delta}_V$	vertical displacement, velocity and acceleration of the mass of the body of the quarter vehicle
ΔP_L	relative pressure between the two chambers of the hydraulic cylinder
$\theta_B, \dot{\theta}_B, \ddot{\theta}_B$	rotation, angular speed and acceleration of the bogie
ω_{SV}	resonance frequency of the amplification of the first stage of the servo valve
ζ_{SV}	damping coefficient of the first stage of amplification of the servo valve